Journal Name

ARTICLE

Linearly Polarized Photoluminescence from an Asymmetric Cyclophane Showing Thermo- and Mechanoresponsive Luminescence

Received 00th January 20xx,
Accepted 00th January 20xx

DOI: 10.1039/x0xx00000x

www.rsc.org/

Yoshimitsu Sagara,*[a,b] Atsushi Seki,[a] Yuna Kim[a] and Nobuyuki Tamaoki*[a]

The first cyclophane to exhibit linearly polarized photoluminescence in the liquid-crystallin and crystalline states is described. An asymmetric cyclophane featuring 4,7-bis(phenylethynyl)-2,1,3-benzothiadiazole group forms a thermodynamically metastable nematic liquid-crystalline phase at room temperature. The compound sandwiched between two glass substrates coated with rubbed polyimide thin layers exhibits homogeneous alignment after shearing. The transition dipole moments of the luminophores align along the rubbing direction. As a result, linearly polarized photoluminescence is achieved at room temperature without any other host materials. Furthermore, the polarized emission is retained after transition to the crystalline phase, which is induced by annealing at 60 °C for 1 h. The cyclophane also shows a thermal and mechanical stimuli-induced change in the photoluminescence colors.

Introduction

A large number of cyclophanes have been investigated to date since [2.2]paracyclophane was reported in 1949.[1] The symmetric and strained character make them fascinating targets in synthetic chemistry and much effort has been devoted to establishing reliable ways to prepare them.[2] The cyclic structures have also attracted much attention from the viewpoint of supramolecular chemistry because the inherent cavity can function as hosts forming inclusive complexes with guest molecules.[2b,2c,3] This association behaviour has been used to achieve various interlocked molecules such as catenanes and rotaxanes.[4] When photoluminescent aromatic groups are incorporated into the cyclic structures, the resultant luminescent cyclophanes exhibit photophysical properties that are different from those of the monomer analogues.[3e,5-12] Furthermore, the photoluminescence colour and/or intensities commonly change upon the intercalation of matching guest molecules or ions. The quantitative modulation of the photoluminescence properties makes the luminescent cyclophanes promising fluorescent probes to evaluate the concentration of guest molecules or ions.

Most of the literature described above has focused on luminescent cyclophanes in solution states where each cyclophane is molecularly dispersed. In contrast, little attention has been paid to luminescent cyclophanes in the solid and/or liquid-crystalline states. Luminescent cyclophanes are intriguing compounds as they may exhibit unconventional photophysical functions that have never been achieved with the acyclic compounds.[10-12] The cyclic structure disturbs the ordered and close-molecular packing, which results in the formation of liquid-crystalline (LC) phases over wide temperature ranges. Even though a number of cyclophanes have been reported to show LC phases,[13,14] their luminescent properties remain unexplored. As LC molecules change the molecular arrangements on LC-LC or LC-crystalline phase transitions, the photoluminescence properties change on the phase transition process.[15] This is because the photoluminescence properties of molecular materials depend on the arrangement of the luminophores inside the material.[15-18] Thus, if external stimuli, such as temperature changes and mechanical forces, can induce phase transitions of luminescent cyclophanes, the photoluminescence properties can be also controlled. Indeed, luminescent cyclophanes having a 1,6-bis(phenylethynyl)pyrene or 9,10-bis(phenylethynyl)anthracene group have been found to exhibit clear photoluminescence colour changes from the supercooled nematic phases to the crystalline phases.[11a,12] Furthermore, the latter cyclophane has been used as an energy acceptor in a triplet–triplet annihilation-based photon upconversion system showing reversible photoluminescence colour changes with thermal stimuli.[12]

Here, we report another attractive feature of luminescent cyclophanes that show LC behaviour as well as external stimuli-responsive luminescence. We demonstrate that an asymmetric cyclophane having a 4,7-bis(phenylethynyl)-2,1,3-benzothiadiazole moiety (Scheme 1) shows a nematic LC phase

[a] Research Institute for Electronic Science, Hokkaido University, N20, W10, Kita-Ku, Sapporo 001-0020, Japan.
[b] JST-PRESTO Honcho 4-1-8, Kawaguchi, Saitama 332-0012, Japan.

Electronic Supplementary Information (ESI) available: Synthesis of compounds **1** and **2**, additional DSC curves, emission decay profiles, XRD patterns and emission images. See DOI: 10.1039/x0xx00000x

at room temperature and exhibits linearly polarized light emission after control of the molecular alignment on the glass substrates with rubbed polyimide layers without any host liquid crystals. Organic materials that exhibit linearly polarized emission have been an intriguing target because of their potential applications such as sophisticated displays[19] and polarised organic light-emitting diodes.[20] Blending luminophores with liquid-crystalline hosts is one of the best way to achieve organic materials with linearly polarized emission character. However, miscibility of the two components sometimes becomes critical issues. To the best of our knowledge, compound **1** is the first example of a luminescent cyclophane that exhibits polarized light emission in the absence of any host liquid crystals. Cyclophane **1** shows a nematic-crystalline phase transition accompanied by a photoluminescence colour change from yellow to green through thermal treatment. Moreover, the latter colour returns to yellow when a mechanical stimulus is applied to the green-emissive crystalline phase. External stimuli-responsive luminescence, as well as stabilization of the disordered LC phases, can be ascribed to the cyclic molecular structure.

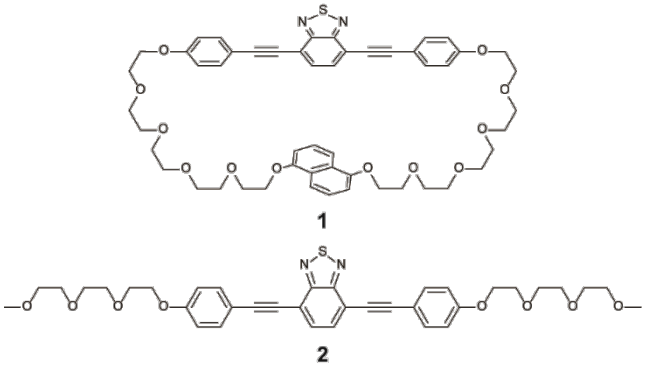

Scheme 1. Molecular structures of cyclophane **1** and the linear reference compound **2**.

Results and discussion

Molecular designs

A 4,7-bis(phenylethynyl)-2,1,3-benzothiadiazole group was selected as the luminescent core of cyclophane **1** because of its relatively high quantum yield.[21] Though some rod-shaped compounds with a 4,7-bis(phenylethynyl)-2,1,3-benzothiadiazole group have been found to show nematic and smectic phases, these acyclic compounds form only crystalline phases at room temperature, which make it difficult for them to achieve a uniaxial alignment of molecules in a large area at room temperature.[22] One naphthalene group was also introduced to the cyclic structure of **1** and the two aromatic moieties were bridged by flexible pentaethyleneglycol chains. The asymmetric cyclic structure was expected to decrease the phase transition temperature from the nematic phase to the highly ordered phases. An acyclic compound **2** bearing the same luminophore was also synthesized as a reference.

Phase transition behaviour

Compound **1**, as expected, shows a nematic phase exhibiting yellow photoluminescence under excitation light of 365 nm in a

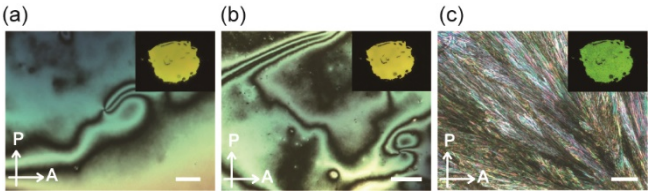

Figure 1. POM images of cyclophane **1** (a) in the nematic phase at 120 °C, (b) in the nematic phase at room temperature, and (c) in the crystalline phase at room temperature. The POM images were taken in the absence of a coverslip. Directions of A: analyzer; P: polarizer. Scale bar: 40 μm. The photoluminescence images of **1** on a quartz substrate are shown in the inset of each POM image. The photoluminescence images were taken under an excitation light of 365 nm in the dark.

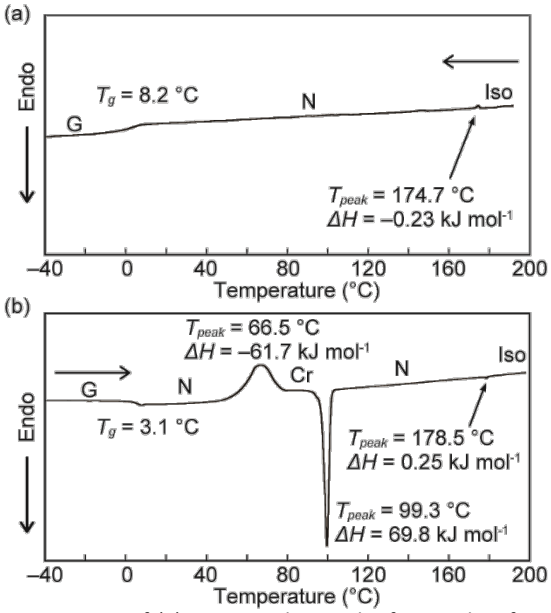

Figure 2. DSC traces of (a) compound **1** on the first cooling from the isotropic state and (b) compound **1** on the first heating from the glassy state. Scanning rate: 5 °C min^{-1}.

wide temperature range on cooling from the isotropic phase (Figure 1, Figure 2a). The polarized optical microscopic (POM) images display a characteristic schlieren texture of a nematic phase both at 120 °C and at room temperature (Figure 1a and 1b). Further cooling results in a glass transition at 8.2 °C without any crystallization (Figure 2a). However, when cyclophane **1** is heated from the glassy phase, a nematic-crystalline phase transition is observed at 66.5 °C (Figure 2b). As the corresponding peak in the DSC trace is exothermic, the nematic phase observed below this temperature is a thermodynamically metastable state. Indeed, after annealing at 60 °C for 1 h, the schlieren texture disappears from the POM observation (Figure 1c), which results from a phase transition from the metastable nematic to the thermodynamically stable crystalline phase. The thermal stimuli-induced crystalline phase exhibits green photoluminescence and displays a phase transition to the

nematic phase at 99.3 °C and a clearing point at 178.5 °C upon further heating (Figure 2b). When compound **1** in the green emissive crystalline state is heated from −40 °C, only two endothermic peaks, which are ascribed to the transition from crystalline to nematic and nematic to isotropic, are observed on the DSC trace (Figure S1a). In keen contrast to **1**, acyclic compound **2** forms a nematic phase in a very narrow temperature range from 86.6 to 82.7 °C on the first cooling (Figure S1b). Furthermore, no nematic phase appeared on the DSC trace of **2** on the second heating. This comparison confirmed that the introduction of cyclic structures is a reliable methodology to enhance liquid-crystallinity.

X-ray diffraction (XRD) patterns (Figure 3) clarified the thermal stimuli-induced phase transition from the thermodynamically metastable nematic phase to the stable crystalline phase. The pattern obtained from cyclophane **1** in the nematic phase at room temperature displays no clear peaks (Figure 3a). In contrast, the crystalline state accessed through annealing at 60 °C for 1 h gives many sharp peaks in the XRD pattern, which reflects the well-ordered crystalline nature (Figure 3b).

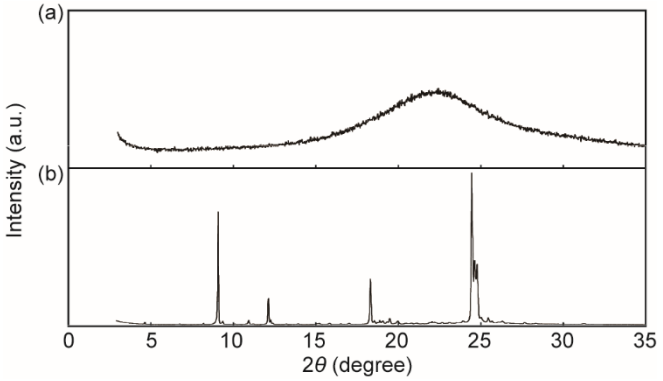

Figure 3. XRD patterns of **1** in the (a) nematic phase and (b) crystalline phase after annealing the nematic phase at 60 °C for 1 h. The patterns were recorded at room temperature.

Photophysical properties in solution

Before investigating the linearly polarized light emission properties, we conducted spectroscopic measurements for the chloroform solution of **1** to obtain the fundamental photophysical properties of an individual molecule. The absorption and photoluminescence spectra of the chloroform solution are shown in Figure 4. A chloroform solution of **1** (c = 1.0×10^{-5} M) presents one absorption band between 350 and 500 nm and another absorption band between 270 and 350 nm. The peak of the former band appears at 437 nm with a molar extinction coefficient of 2.7×10^4 L mol^{-1} cm^{-1}. The absorption band of linear compound **2** (gray line) is very similar to that of compound **1**. As shown in Figure 4b, the chloroform solution of **1** displays a broad emission band with the maximum at 557 nm. The emission band of **2** is slightly blue-shifted compared with that of **1**, which results from non-negligible electronic ground-state interactions between two aromatic groups in cyclophane **1**. This is supported by the emission lifetime measurement (Figure 5). The emission decay profile recorded for the chloroform solution of **2** could be fitted to a single exponential decay function and only one emission lifetime of 6.0 ns is obtained, while cyclophane **1** in chloroform gives an emission decay profile that is fitted to a bi-exponential decay function and gives two emission lifetimes of 0.5 and 4.6 ns. Furthermore, the emission quantum yield of **1** in chloroform (Φ = 0.15) is much lower than that of linear compound **2** (Φ = 0.99).

Thermoresponsive luminescence

Next, we also examined the thermal stimuli-responsive luminescence behaviour of cyclophane **1** in the condensed state. As shown in Figure 6, the photoluminescence spectrum of compound **1** in the nematic phase at room temperature shows a maximum at 565 nm. Because the emission band of the luminophore strongly

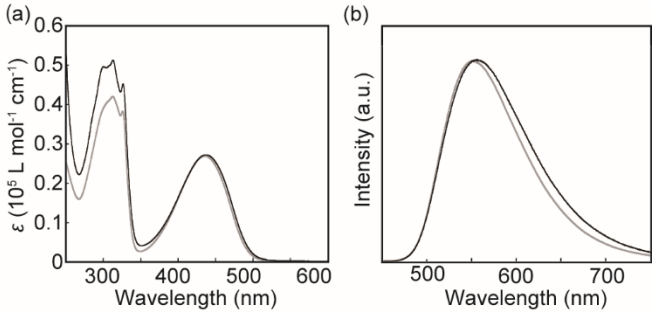

Figure 4. (a) Absorption and (b) photoluminescence spectra of the chloroform solutions of cyclophane **1** (black line) and the reference compound **2** (gray line) (c = 1.0×10^{-5} M). All spectra were recorded at room temperature. Photoluminescence spectra were obtained with an excitation light of 400 nm.

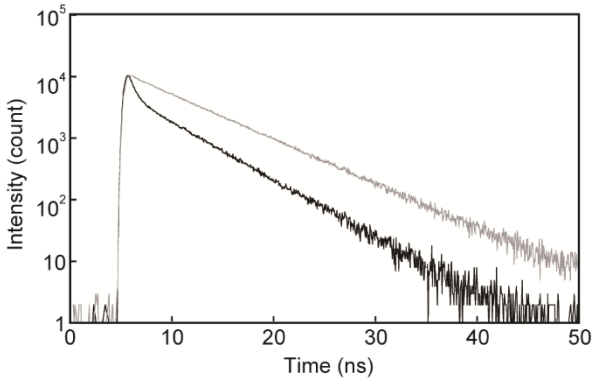

Figure 5. Emission decay profiles of cyclophane **1** (black line) and compound **2** (gray line) in chloroform. The profiles were monitored at 550 nm at room temperature with excitation light of 405 nm.

depends on environmental polarity,[23] we were unable to consider the emission from the nematic phase as monomer emission based on the fact that the emission band appears in a similar wavelength region to that of the chloroform solution. The spectrum of cyclophane **1** shows a significant blue shift after annealing at 60 °C for 1 h ($\lambda_{em,max}$ = 536 nm), which coincides with the color change shown in Figure 1. The emission quantum yield also changes from 0.28 to 0.32 on the nematic to crystalline phase transition. The quantum yields are

higher than that of solution because the non-radiative decay pathway is restricted owing to the suppression of the intramolecular motion at the luminophore in the condensed states. Emission lifetime measurements were also performed for both phases to obtain more insight into the thermoresponsive luminescent behaviour (Figure 7). The emission decay profiles recorded for the nematic and crystalline phases could be fitted to tri-exponential and bi-exponential decay functions, respectively. A relatively longer emission lifetime of 7.9 ns is observed for the nematic phase, whereas such longer-lived emissive species are not observed for **1** in the crystalline phase (1.9 and 4.1 ns). Because the latter emission lifetimes are similar to those of the monomeric state of **1** in chloroform, we proposed that the luminophores in the crystalline state are in a monomer-like environment. The emissive species with a long lifetime observed for the nematic phase could be ascribed to the associated state of the luminophores owing to the low-ordered nature of the nematic liquid crystals.

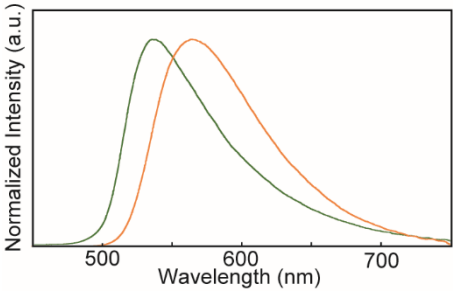

Figure 6. Photoluminescence spectra of **1** in the nematic phase (orange line) and the crystalline state that was accessed thorough annealing (green line). All spectra were recorded at room temperature with an excitation light of 400 nm.

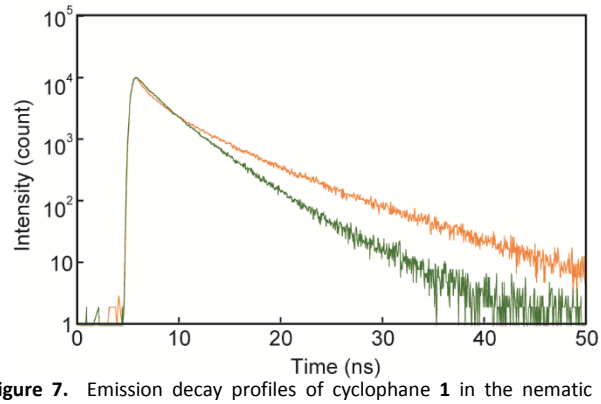

Figure 7. Emission decay profiles of cyclophane **1** in the nematic phase (orange line) and in the crytalline phase (green line). The profiles were monitored at 550 nm at room temperature with excitation light of 405 nm.

Linearly polarized emission

As cyclophane **1** was found to show the nematic phase at room temperature, we investigated the uniaxial alignment control and linearly polarized light emission in the nematic phase of compound **1** at room temperature (Figure 8). Compound **1** in the nematic phase was sandwiched between two glass substrates with rubbed polyimide surfaces. After compound **1** between the substrates were sheared along the rubbing direction at 120 °C and subsequent cooled to room temperature, a homogeneous texture of the nematic phase was observed on the POM observation (Figure 8a). An absorption spectroscopic measurement clarified the transition dipole moment, which is parallel to the long axis of the luminophore of **1**,[24] aligns along the rubbing direction (Figure 8b). Although the scattering increases the baselines, the polarized absorbances parallel and perpendicular to the rubbing direction are 0.9 and 0.55 at 437 nm, respectively. The observed difference in absorbance is smaller than that of the reported nematic liquid crystal doped with a rod-shaped compound having the same luminophore (0.25 mol%).[24] This is ascribed to the cyclic molecular structure of compound **1**. The rod-shaped compound can easily align in the nematic LC host. Whereas in the case of compound **1**, the cyclic structure disturbed the well-ordered molecular assemblies leading to a larger distribution of directors, and consequently the smaller absorbance difference. As shown in Figure 8c, the aligned cyclophane **1** in the nematic phase clearly shows linearly polarized photoluminescence under an excitation light of 365 nm. This is the first example of cyclophanes that show a linearly polarized light emission. The ratio of the photoluminescence intensity is 2.9 at the peak of 564 nm in the direction parallel and perpendicular to the rubbing direction, and the ratio does not significantly change between 530 and 650 nm (Figure S2a). After the thermal stimuli-induced phase transition to the crystalline state, the emission band showed a blue shift and the polarized photoluminescence was still observed (Figure 8d). However, the ratio described above decreases to 1.7 and this value is maintained over the wavelength range from 530 to 650 nm (Figure S2b). This implies that the crystallization process disturbed the well-aligned structures which are readily achieved in the nematic phase.

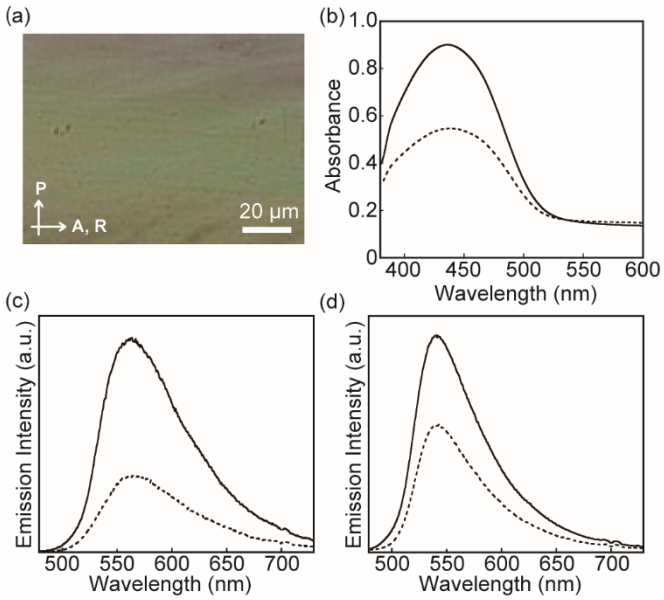

Figure 8. (a) POM image of cyclophane **1** sandwiched between glass substrates with rubbed polyimide thin layers. Cyclophane **1** is in the nematic phase. Directions of A: analyzer; P: polarizer; R: rubbing. (b) Absorption spectra recorded in the direction parallel (solid line) and

perpendicular (dotted line) to the rubbing direction. (c,d) Polarized photoluminescence spectra of **1** in the nematic phase (c) and the crystalline phase accessed through an annealing process (d). The polarized emission spectra were recorded in the direction parallel (solid line) and perpendicular (dotted line) to the rubbing direction with an excitation light of 365 nm. All spectra were measured at room temperature.

Mechanoresponsive Luminescence

It is noteworthy that the mechanical stimulus also changes the photoluminescence color of **1** in the crystalline state that was obtained after annealing at 60 °C for 1 h to the nematic phase. When a mechanical stimulus is applied to the crystal of compound **1** at room temperature, the photoluminescence color changes from green to yellow (Figure 9). The photoluminescence spectrum showed a red shift and an emission peak was observed at 571 nm (Figure 10), which is similar to that of the nematic phase. The emission decay profile (Figure S3) is also similar to that of **1** in the nematic phase. The obtained curve could be fitted to a tri-exponential decay function and gave an emission lifetime of 6.8 ns. This is ascribed to luminophores in the associated state as observed in the nematic phase. These data suggest that mechanical stimuli lead to a low-ordered state compared with the crystalline states, though XRD measurements were not able to be performed owing to the rapid recovery to the initial crystalline states. After the recovery, the compound **1** gave several X-ray diffraction peaks at the same positions as those for the initial crystalline phase (Figure S4). Furthermore, this recovery process is highly temperature dependent. As shown in Figure S5, mechanical stimuli-induced yellow emissive part still can be seen after 5 min when the ground sample was kept at 15 °C. In contrast, putting a ground sample on a hot stage kept at 40 °C results in immediate recovery of the initial green emission (Figure S5f). The temperature dependent character observed here was similar to that found for a pyrene-based asymmetric cyclophane in our previous study.[11a]

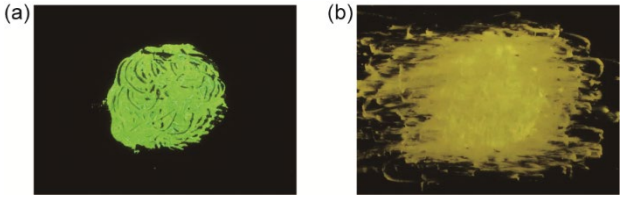

Figure 9. Images documenting the mehcanical stimuli-induced change in photoluminescence color of **1** at room temperature. (a) Compound **1** in the crystalline phase before grinding. (b) Compound **1** after grinding at room temperature. The images were taken on quartz substrates under excitation light at 365 nm.

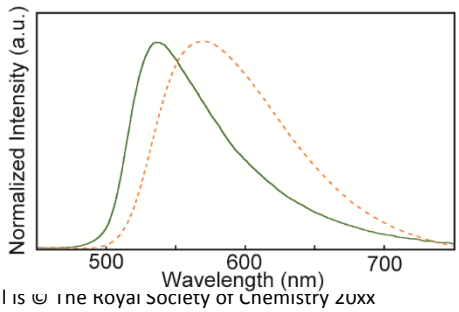

Figure 10. Photoluminescence spectra of **1** in the crystalline state (green solid line) and in the ground state (orange dotted line). All spectra were measured at room temperature (λ_{ex} = 400 nm).

Conclusions

In conclusion, we demonstrate that an asymmetric benzothiadiazole-based cyclophane **1** exhibits linearly polarized photoluminescence as well as thermo- and mechano-responsive luminescence in the condensed state. The cyclic character disturbs the ordered molecular packing, which leads to the nematic LC phase at room temperature. Since compound **1** shows a phase transition to the crystalline phase through thermal treatment, the nematic phase is a thermodynamically metastable state. A homogeneous alignment is obtained when the cyclophane is sandwiched between glass substrates with rubbed polyimide thin layers. The transition dipoles are aligned parallel to the rubbing direction. Consequently, linearly polarized emission is achieved and remains after a transition to the crystalline states. To the best of our knowledge, this is the first example of cyclophanes showing linearly polarized emission. The molecular design strategy adopted in this study may be general and result in a number of less-ordered molecular assemblies that can provide unconventional photophysical functions and stimuli-responsive behaviour.

Experimental Section

General methods and materials

All reagents and solvents were purchased from Tokyo Kasei, Wako, and Aldrich. All reactions were carried out under nitrogen atmosphere. Silica gel column chromatography was carried out with a Biotage Isolera Flash system. ^{1}H NMR spectra were measured with a JEOL JNM-ECX 400 spectrometer and all chemical shifts are quoted in ppm relative to the signal of tetramethylsilane (δ = 0.00) as an internal standard. ^{13}C NMR spectra were measured with a JEOL JNM-ECX 400 spectrometer and all chemical shifts (δ) are quoted in ppm using residual solvents of $CDCl_3$ (δ = 77.16) and DMSO (δ = 39.52) as the internal standard. Coupling constants (J) are reported in Hz and relative intensities are also shown. Matrix-assisted laser desorption ionization time-of-flight (MALDI-TOF) mass spectra were recorded on an AB SCIEX TOF/TOF 5800. High resolution electrospray ionization (ESI) mass spectra were obtained on a Thermo Scientific Exactive. Elemental analysis was conducted with an Exeter Analytical CE440 Elemental Analyzer. The DSC measurements were carried out using a Hitachi DSC 7020 with a heating/cooling rate of 5 ˚C/min under nitrogen atmosphere. Powder X-ray diffraction measurements were conducted with a Rigaku

SmartLab. UV-vis absorption spectra were recorded with a JASCO V-550. Steady-state fluorescence spectra were measured on a JASCO FP-6500. Time-resolved fluorescence measurements were conducted with a Hamamatsu Photonics Quantaurus-Tau. Quantum efficiencies of compounds in solution were calculated using Rhodamine 6G in EtOH (Φ = 0.95) as the reference. Quantum efficiencies for solid samples were measured with a Hamamatsu Photonics Quantaurus-QY. Polarized optical microscopic observations were carried out with an Olympus BX-60 optical microscope equipped with a Sony DXC-950 3CCD camera. An AS ONE hot plate NA-1 was used for the thermal treatment. Linear Polarizer Film was purchased from MeCan Imaging Inc.. Emission images were taken with Canon EOS 9000D.

Linearly polarized photoluminescence measurements

For the linearly polarized photoluminescence measurements, mechanically rubbed polyimide (PI)-coated glass substrates were used. The glass substrates were washed with methanol and dried before preparing the alignment layer. The PI precursor solutions (SE-150) and thinner solvent (26 thinner) were purchased from Nissan Chemical Industries, Ltd. A solution of PI varnish was mixed with the thinner at a ratio of 1/2 (wt/wt). The mixture of the PI precursor was spun on the glass substrates at the rate of 1500 rpm for 50 s. After the spincoated glass substrates were prebaked on the hot plate for 1 hour at 180 °C, the substrates were baked at 200 °C for 1 hour. The prepared PI surface was rubbed in one direction by using a nonwoven fabric.

The linearly polarized photoluminescence measurement was carried out by using an Ocean Optics QEPro equipped with a R400-7-VIS-NIR reflectance probe as emission light detector. The excitation light source was a Handy UV lamp AS ONE SLUV-4 (excitation wavelength: 365 nm). The sample LC cell and the light source were set on the stage. The incident angle of the excitation light to the sample was tuned to approximately 45 degrees. The detector was placed in the appropriate position where reflection of the excitation UV light was not detected.

Conflicts of interest

There are no conflicts to declare.

Acknowledgements

We thank Prof. Y. Urano for emission quantum yield measurements. This work was supported by JSPS KAKENHI Grants JP16H00818 and JP18H02024, the Futaba Electronics Memorial Foundation, the Kurita Water and Environment Foundation, and the Foundation Advanced Technology Institute.

Notes and references

1 C. J. Brown and A. C. Farthing, *Nature*, 1949, **164**, 915-916.
2 (a) D. J. Cram and J. M. Cram, *Acc. Chem. Res.*, 1971, **4**, 204-213; (b) C. Seel and F. Vögtle, *Angew. Chem. Int. Ed.*, 1992, **31**, 528-549; (c) J. O. Jeppesen, M. B. Nielsen and J. Becher, *Chem. Rev.*, 2004, **104**, 5115-5132; (d) P. G. Ghasemabadi, T. Yao and G. J. Bodwell, *Chem. Soc. Rev.*, 2015, **44**, 6494-6518.
3 (a) R. M. Izatt, K. Pawlak, J. S. Bradshaw and R. L. Bruening, *Chem. Rev.*, 1995, **95**, 2529-2586; (b) F. P. Schmidtchen and M. Berger, *Chem. Rev.*, 1997, **97**, 1609-1646; (c) A. Jasat and J. C. Sherman, *Chem. Rev.*, 1999, **99**, 931-968; (d) E. A. Meyer, R. K. Castellano and F. Diederich, *Angew. Chem. Int. Ed.*, 2003, **42**, 1210-1250; (e) D. Ramaiah, P. P. Neelakandan, A. K. Nair and R. R. Avirah, *Chem. Soc. Rev.*, 2010, **39**, 4158-4168; (f) M. Xue, Y. Yang, X. Chi, Z. Zhang and F. Huang, *Acc. Chem. Res.*, 2012, **45**, 1294-1308.
4 (a) D. B. Amabilino and J. F. Stoddart, *Chem. Rev.*, 1995, **95**, 2725-2828; (b) V. Balzani, M. Gómez-López and J. F. Stoddart, *Acc. Chem. Res.*, 1998, **31**, 405-414; (c) A. R. Pease, J. O. Jeppesen, J. F. Stoddart, Y. Luo, C. P. Collier and J. R. Heath, *Acc. Chem. Res.*, 2001, **34**, 433-444; (d) I. Aprahamian, O. Š. Miljanic, W. R. Dichtel, K. Isoda, T. Yasuda, T. Kato and J. F. Stoddart, *Bull. Chem. Soc. Jpn.*, 2007, **80**, 1856-1869; (e) A. C. Fahrenbach, C. J. Bruns, D. Cao and J. F. Stoddart, *Acc. Chem. Res.*, 2012, **45**, 1581-1592; (f) Y. Okumura and K. Ito, *Adv. Mater.*, 2001, **13**, 485-487; (g) S. Erbas-Cakmak, D. A. Leigh, C. T. McTernan and A. L. Nussbaumer, *Chem. Rev.*, 2015, **115**, 10081-10206; (h) V. Balzani, A. Credi, F. M. Raymo and J. F. Stoddart, *Angew. Chem. Int. Ed.*, 2000, **39**, 3348-3391; (i) S. F. M. van Dongen, S. Cantekin, J. A. A. W. Elemans, A. E. Rowan and R. J. M. Nolte, *Chem. Soc. Rev.*, 2014, **43**, 99-122.
5 (a) O. Baudoin, F. Gonnet, M.-P. Teulade-Fichou, J.-P. Vigneron, J.-C. Tabet and J.-M. Lehn, *Chem. Eur. J.*, 1999, **5**, 2762-2771; (b) M.-P. Teulade-Fichou, J.-P. Vigneron and J.-M. Lehn, *J. Chem. Soc., Perkin Trans. 2*, 1996, 2169-2175; (c) P. Cudic, M. Zinic, V. Tomisic, V. Simeon, J.-P. Vigneron and J.-M. Lehn, *J. Chem. Soc., Chem. Commun.*, 1995, 1073-1075.
6 (a) P. P. Neelakandan, K. S. Sanju and D. Ramaiah, *Photochem. Photobiol.*, 2010, **86**, 282-289; (b) P. P. Neelakandan and D. Ramaiah, *Angew. Chem. Int. Ed.*, 2008, **47**, 8407-8411.
7 (a) H. Abe, Y. Mawatari, H. Teraoka, K. Fujimoto and M. Inouye, *J. Org. Chem.*, 2004, **69**, 495-504; (b) M. Inouye, K. Fujimoto, M. Furusyo and H. Nakazumi, *J. Am. Chem. Soc.*, 1999, **121**, 1452-1458.
8 L. Qiu, C. Zhu, H. Chen, M. Hu, W. He and Z. Guo, *Chem. Commun.*, 2014, **50**, 4631-4634.
9 P. Spenst and F. Wurthner, *Angew. Chem. Int. Ed.*, 2015, **54**, 10165-10168.
10 P. C. Nandajan, P. P. Neelakandan and D. Ramaiah, *RSC Adv.*, 2013, **3**, 5624.
11 (a) Y. Sagara, C. Weder and N. Tamaoki, *Chem. Mater.*, 2017, **29**, 6145-6152; (b) Y. Sagara and N. Tamaoki, *RSC Adv.*, 2017, **7**, 47056-47062; (c) Y. Sagara, C. Weder and N. Tamaoki, *RSC Adv.*, 2016, **6**, 80408-80414; (d) Y. Sagara, Y. C. Simon, N. Tamaoki and C. Weder, *Chem. Commun.*, 2016, **52**, 5694-5697.
12 K. Mase, Y. Sasaki, Y. Sagara, N. Tamaoki, C. Weder, N. Yanai and N. Kimizuka, *Angew. Chem. Int. Ed.*, 2018, **57**, 2806-2810.
13 (a) V. Percec, P. J. Turkaly and A. D. Asandei, *Macromolecules*, 1997, **30**, 943-952; (b) V. Percec and A. D. Asandei, G. Ungar, *Chem. Mater.*, 1996, **8**, 1550-1557; (c) V. Percec, A. D. Asandei and P. Chu, *Macromolecules*, 1996, **29**, 3736-3750; (d) V. Percec, M. Kawasumi, P. L. Rinaldi and V. E. Litman, *Macromolecules*, 1992, **25**, 3851-3861.
14 (a) T. Hegmann, B. Neumann, R. Wolf and C. Tschierske, *J. Mater. Chem.*, 2005, **15**, 1025-1034; (b) B. Neumann, T. Hegmann, C. Wagner, P. R. Ashton, R. Wolf and C. Tschierske, *J. Mater. Chem.*, 2003, **13**, 778-784; (c) B. Neumann, T. Hegmann, R. Wolf and C. Tschierske, *Chem. Commun.*, 1998, 105-106; (d) B. Neumann, D. Joachimi and C. Tschierske, *Adv. Mater.*, 1997, **9**, 241-244.

15 (a) Y. Sagara, S. Yamane, M. Mitani, C. Weder and T. Kato, *Adv. Mater.*, 2016, **28**, 1073-1095; (b) S. Yamane, K. Tanabe, Y. Sagara and T. Kato, *Top. Curr. Chem.*, 2012, **318**, 395-405; (c) Y. Sagara and T. Kato, *Nat. Chem.*, 2009, **1**, 605-610.
16 (a) K. Araki, T. Mutai, *Photochemistry*, 2016, **43**, 191-225; (b) J. Mei, N. L. C. Leung, R. T. K. Kwok, J. W. Y. Lam, B. Z. Tang, *Chem. Rev.*, 2015, **115**, 11718-11940; (c) S. S. Babu, V. K. Praveen, A. Ajayaghosh, *Chem. Rev.*, 2014, **114**, 1973-2129; (d) F. Würthner, C. R. Saha-Möller, B. Fimmel, S. Ogi, P. Leowanawat, D. Schmidt, *Chem. Rev.*, 2016, **116**, 962-1052; (e) S. Yagai, *Bull. Chem. Soc. Jpn.*, 2015, **88**, 28-58.
17 (a) Z. Ma, Z. Wang, M. Teng, Z. Xu and X. Jia, *Chemphyschem*, 2015, **16**, 1811-1828; (b) Z. Chi, X. Zhang, B. Xu, X. Zhou, C. Ma, Y. Zhang, S. Liu and J. Xu, *Chem. Soc. Rev.*, 2012, **41**, 3878-3896; (c) X. Zhang, Z. Chi, Y. Zhang, S. Liu, J and Xu, *J. Mater. Chem. C*, 2013, **1**, 3376-3390; (d) K. Ariga, T. Mori and J. P. Hill, *Adv. Mater.*, 2012, **24**, 158-176.
18 (a) F. Ciardelli, G. Ruggeri and A. Pucci, *Chem. Soc. Rev.*, 2013, **42**, 857-870; (b) A. P. Haehnel, Y. Sagara, Y. C. Simon and C. Weder, *Top. Curr. Chem.*, 2015, **369**, 345-375; (c) C. Calvino, L. Neumann, C. Weder and S. Schrettl, *J. Polym. Sci., Part A: Polym. Chem.*, 2017, **55**, 640-652.
19 C. Weder, C. Sarwa, A. Montali, C. Bastiaansen, P. Smith *Science*, 1998, **279**, 835-837.
20 Y. Wang, J. Shi, J. Chen, W. Zhu and E. Baranoff, *J. Mater. Chem. C*, 2015, **3**, 7993-8005.
21 B. A. DaSilveira Neto, A. S. A. Lopes, G. Ebeling, R. S. Gonçalves, V. E. U. Costa, F. H. Quina and J. Dupont, *Tetrahedron*, 2005, **61**, 10975-10982.
22 A. A. Vieira, R. Cristiano, A. J. Bortoluzzi and H. Gallardo, *J. Mol. Struct.*, 2008, **875**, 364-371.
23 Y. Sagara, M. Karman, E. Verde-Sesto, K. Matsuo, Y. Kim, N. Tamaoki and C. Weder, *J. Am. Chem. Soc.*, 2018, **140**, 1584-1587.
24 P. Alliprandini Filho, G. G. Dalkiranis, R. A. S. Z. Armond, E. M. Therezio, I. H. Bechtold, A. A. Vieira, R. Cristiano, H. Gallardo, A. Marletta and O. N. Oliveira, *PCCP*, 2014, **16**, 2892-2896.